COMPARISON OF FOUR TYPES OF RADIAL TURBINES FOR A 250KW ORC POWER INSTALLATION

Maksim Smirnov[1]*, Natalia Kuklina[2], Aleksandr Sebelev[1], Alessandro Zuccato[2] and Nikolay Zabelin[1]

[1]Peter the Great St. Petersburg Polytechnic University (SPbPU), St. Petersburg, Russia

[2]Zuccato Energia Srl, via della Consortia 2, Verona, Italy

*Corresponding Author: m.smirnov.turbo@gmail.com

ABSTRACT

This paper seeks to compare four solutions for an ORC power plant rated at 250 kW running with R1233zdE as the working fluid: a radial inflow – axial outflow turbine with a typical reaction about of 0.5, radial centripetal turbines with reaction of 0.36 and 0.05 and an impulse centrifugal turbine. All these turbines are single stage and high-speed. Steady state CFD simulations were carried out to assess the performance and the axial force values at the design and partial load.

As expected, the radial inflow turbine has exhibited the best performance, followed then by the centripetal reaction turbine with 4% of a relative efficiency decrease. Both impulse turbines have shown 11% less efficiency at the design point comparing to the radial inflow stage. Under the partial load, the turbines have exhibited different trends of their efficiency behaviour. In particular, with a power output reduction from 100 to 40%, the radial inflow and the centripetal turbine have lost 8% of their efficiency, while the centripetal impulse turbine has lost 17% and the centrifugal impulse turbine just 5%.

The axial force of the radial inflow and both centripetal stages may be balanced to reach a desired value by means of the modification of the disk back seal. Instead, the centrifugal impulse stage fails to provide such a balancing, which results in high values of the axial thrust even despite an impulse nature of this stage.

1 INTRODUCTION

Typically, the radial inflow turbines are used as turbine expanders in microturbomachinery. This is due to their high efficiency even with small volumetric flows and a lower clearance-sensitivity because of the centripetal component $(u^2_1 - u^2_2)/2$ of the Euler work. However, in the recent years noticeable interest has raised also to other turbine types as candidate solutions for the ORC expanders at low power output range. The literature review provided below concerns these candidate solutions, specifying the turbine design parameters and the reference values of their efficiency. The turbines mentioned in the review had different pressure ratios and were designed for different working fluids. However, typical ranges of the total-to-static efficiency for each turbine type were discovered: from 73 to 80% for the centripetal impulse stages, from 81 to 85% for the centrifugal stages and up to 87% for the radial inflow stages. The results obtained by the authors of this paper are also within the abovementioned ranges.

1.1 Radial inflow – axial outflow centripetal stages (Radial Inflow turbines)

Radial inflow turbine is a common turbine type in modern small power scale ORCs. As an advantage, it may provide total-to-static efficiencies up to 87% (Klonowicz *et al.* 2015). As a drawback, the turbine normally has a reaction degree of about 0.5, which generates considerable thrust and requires high rotational speed. Significant manufacturing efforts are attributed to the impeller trailing edge and finishing of the hub surface due to relatively long blades at the outlet part. This fact leads to high cost of radial inflow impellers.

1.2 Radial inflow – radial outflow centripetal stages (Centripetal or cantilever turbines)

Bavarian scientists have studied experimentally the performance of "quasi-impulse" cantilever single-stage turbine (Weiß *et al*., 2017; Weiß *et al*., 2018) with pressure ratio of about 20. The maximum efficiency reached by the stage was in the range from 73 to 77%. Bülten *et al.* (2013) in their paper described design, simulation, experimental tests and subsequent optimization of 70 kW ORC prototype based on a centripetal "quasi-impulse" cantilever single-stage turbine. The turbine had a significant pressure ratio of 60, which in combination with a small power output caused high design rotational speed of 30 000 rpm. The first tested turbine has exhibited total-to-static efficiency about 70%, while after its optimization CFD simulations predicted an efficiency increase by 10% absolute.

1.3 Radial inflow – radial outflow centrifugal stages (Centrifugal turbines)

Radial outflow machines found their place in ORC applications mostly because of a good match between the area increase and the volumetric flow rise while moving radially outwards. This enables to avoid significant increase of the blade height along the flow path with related design and manufacturing simplifications.

Shanghai scientists Liu and Huang (2018) designed and simulated 15 kW radial centrifugal impulse turbine, which efficiency exceeded 85% in accordance with the CFD simulations. Song *et al.* (2017) compared one, two and three-stage centrifugal turbines rated at 330 kW. Single stage configuration provided total-to-static efficiency of 82.7% as a result of the CFD simulations. Korean scientists (Kim and Kim 2020) performed the preliminary design and simulation of a 400 kW centrifugal ORC turbine including its off-design performance analysis. The machine reached total-to-static efficiency of about 85% at its design point.

1.4 Axial turbines

Moroz *et al.* 2013 studied an axial reaction turbine to employ it as an expander for a low-temperature ORC installation driven by R245fa. The final design equipped with an outlet diffuser has exhibited $\eta_{t\text{-}s}$ of 81.8%. The contribution of the diffuser into the performance improvement was as high as 3%. As shown, an axial reaction turbine even designed for a limited pressure ratio of 5 was getting pretty complex to exceed 80% of the efficiency, having required a diverging meridional section, a shroud and a diffuser with an exhaust cone bearded by the struts.

1.5 Existing studies on the comparison of performance of different turbine types for the ORCs

Weiß *et al*. (2018) studied both numerically and experimentally an axial impulse and a cantilever radial impulse turbine at both design and off-design points. The capability of the radial turbine to surpass the efficiency of the axial one was demonstrated. Klonowicz *et al.* (2015) designed and simulated numerically 500 kW ORC turbines driven by MDM, one of them was an axial multistage turbine rotating at 3 000 rpm, while another one was a radial inflow high-speed single stage turbine. Having shown better total-to-static efficiency (91.2% versus 86.6% for the radial inflow turbine), the multistage axial turbine however required much more manufacturing efforts since it consisted of 10 stages. Al Jubori *et al.* (2017) compared numerically an axial and a centrifugal reaction turbine of a micro-ORC rated at 15 kW. Turbines designed for n-Pentane reached total-to-total efficiency of 82.5% and 79%, respectively.

2 SCOPE OF THE STUDY

Despite numerous studies on the performance evaluation of the ORC turbines, including their part-load operation, very few of them are considering the turbine axial thrust. However, as shown by Moroz *et al*. (2013), limitations arising from the bearings capabilities may require significant redesign efforts and cause efficiency penalties. Therefore, the axial thrust evaluation is a crucial part of the turbine preliminary design process.

So, the first goal of the current study is to perform a joint performance-thrust evaluations at the design and off-design regimes. Secondly, the paper seeks to provide a comparison of four types of radial

stages employed at the same boundary conditions, since before axial and radial turbines only were cross-compared and not two or more radial turbines between each other. Finally, the paper provides examples of the turbines running with R1233zdE, a promising low-GWP alternative to the existing ORC fluids. Authors hope that the results of the study may facilitate making reasonable choices during the preliminary design phase.

3 STUDIED TURBINES

Four radial turbines of different types are designed for the comparison in this study: a radial inflow, a centripetal reaction, a centripetal impulse, a centrifugal turbine. Axial turbine is excluded deliberately from considerations since appears to be more complex in terms of the mechanical design to approach high efficiency within the power output range in question. All the radial turbines are designed for the same boundary conditions, specified in table 1. During the design procedure, a simple in-house 1D meanline tool was used. Then, each stage was simulated numerically for the fine-tuning. In doing so, the blade heights were adjusted to reach the design reaction, the nozzle and the impeller contouring was corrected to eliminate as far as possible the pressure shocks and the flow separations. Table 2 summarizes turbines' geometrical characteristics and operating condition.
The differences between the centripetal turbines are to be highlighted: they were designed for different reactions, therefore, the required rotational speed, the impeller diameters and the blade heights were completely different. In the centripetal impulse turbine the impeller diameters were selected so as to keep the impeller blade height constant over the radius ($l_2=l_1$).

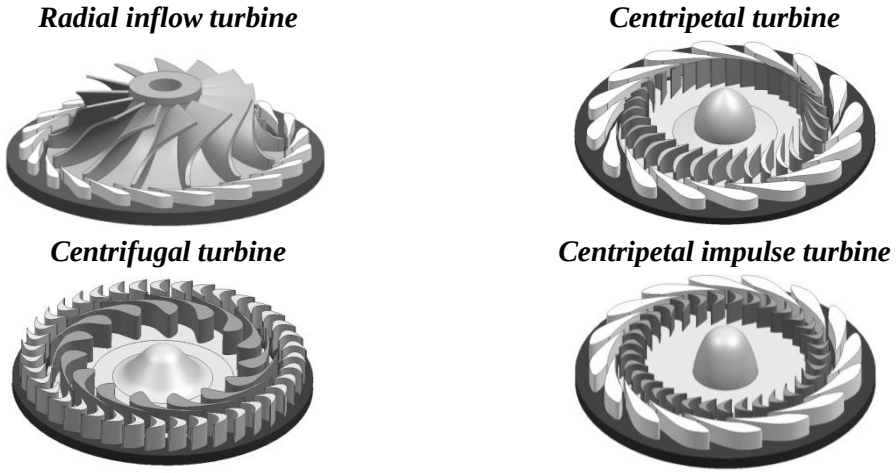

Figure 1: Studied turbine stages

Table 1: Boundary conditions

Inlet total pressure, MPa	Inlet total temperature, K	Outlet static pressure, MPa
2.45	433.15 (160°C)	0.275

4 SIMULATION APPROACH

4.1 CFD simulation method

ANSYS CFX 17.0 was used for the numerical simulation. Mixing plane rotor-to-stator interface was used, therefore only one sector of the nozzle and the impeller were included into the model with the periodic boundary conditions. $y+$ parameter were kept in the range $30< y+ <45$. High resolution advection scheme was used in the simulation. Steady state approach was applied with automatic timescale option. The timescale factor of 0.7 was set to facilitate the convergence while simulating the off-design points. The same CFD approach was employed by Bülten *et al.* (2013) and demonstrated good agreement with the experimental data for a centripetal ORC turbine. Mesh sensitivity study was

not performed specifically for the studied stages but the results obtained by Sebelev *et. al* (2015) was applied. In accordance with this data, 1.15 mln of nodes per each blade sector were sufficient to get the grid independent solution for the stage with the maximum Mach number of 2.6. Aungier Redlich-Kwong equation of state was used. Sebelev *et al.* (2019) compared this equation of state with accurate Span-Wagner equation and found a difference in the calculation of the properties less than 6% within the pressures up to $1.1p_{cr}$. Therefore, Aungier Redlich-Kwong equation is able to provide satisfactory accuracy and, in the same time, good simulation convergence due to its simplicity. Ideal gas specific heat capacity coefficients, required by Aungier Redlich-Kwong equation of state to calculate the real gas heat capacities, were obtained with using Refprop (Mondejar *et al.* 2015). The convergence criteria for the steady-state solutions were: 1) RMS residuals less than 10^{-5}; 2) imbalances less than 0.5%; 3) fluctuations of the turbine efficiency and power output less than 1%.

Table 2: Turbines' geometrical characteristics and operating conditions

Parameters	Dimensions	Radial inflow turbine	Centripetal turbine	Centripetal impulse turbine	Centrifugal turbine
Reaction ρ	-	0.5	0.36	0.05	0.05
Rotational speed n	rev/min	24500	21500	16000	21000
Impeller inlet diameter d_1	mm	160	160	170	130
Impeller outlet mean diameter d_2	mm	86	125	130	172
Nozzle outlet blade height l_1	mm	8.5	10.2	19	16.4
Impeller outlet blade height l_2	mm	35.5	26	19	16.4
Shroud	-	no	yes	no	no
Shroud hot running clearance	mm	0.15	0.2	0.15	0.15

4.2 Axial thrust assessment

The axial force developed by the turbines was assessed numerically. In order to do this impeller disk's cavities were included into the model. The thrust magnitudes were calculated on the surfaces of the impeller disk and blades with using the corresponding function of Ansys CFD Post. The centripetal turbines had labyrinth seal at the disk's back side, aimed at decreasing the leakage flow and balancing the axial force. It included 12 fins with 0.25 mm clearance at the running (hot) conditions. The simulation domains with the settings imposed are presented in figure 2. For the centrifugal turbine, unloading holes implemented for the thrust relief also were simulated. CFD simulations with using k-ω SST turbulence model for the axial force evaluations were validated by Finnish scientists (Tiainen *et al.* 2021) and showed an acceptable agreement with the experimental measurements, underestimating the thrust by 5-30%.

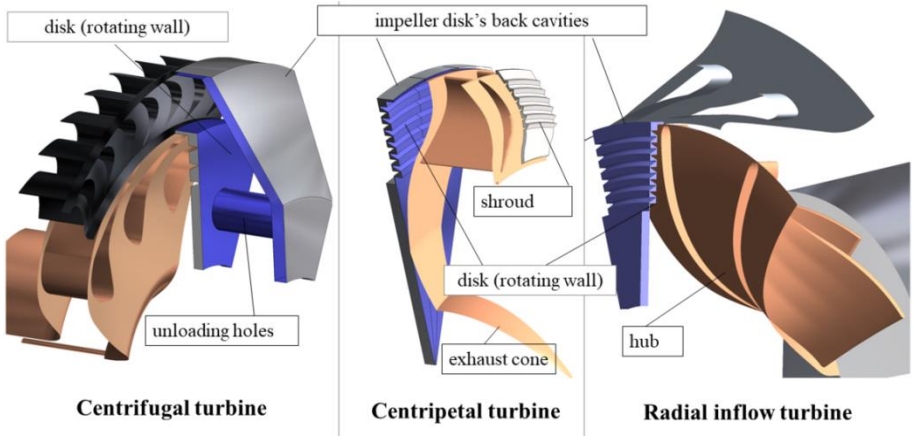

Figure 2: Simulation domains

5 DISCUSSIONS

5.1 Power and efficiency at the design load

As was expected, the radial inflow turbine exhibited the best efficiency with the power output of 297.8 kW. The centripetal reaction turbine was less efficient by 4% (relative) with the power output of 283.3 kW. The centrifugal turbine at the design point had a poor efficiency which was 11% less and showed the power output decrease by 33.6 kW as compared to the radial inflow turbine. The same performance was demonstrated by the centripetal impulse turbine, which generated 262.6 kW only at its design point.

One of the reasons of the better efficiency of the radial inflow turbine is the contribution of the outlet diffuser, which was as high as 6 kW or 1.8% of the efficiency. In this turbine configuration the diffuser is increasing the stage enthalpy drop, while in the centripetal stage the diffuser cannot be applied. Moreover, in the centripetal stage the exhaust flow's turn from radial to axial direction generated pressure losses. As a result, the effective enthalpy drop on the radial inflow stage exceeded the one on the centripetal stages by 6%, which was reflected in their different performance. Concerning the centrifugal stage, its outlet part naturally acts like a diffuser, however, this impact should be studied in details also considering the resistance of the outlet volute or hood.

In order to visualize the flow field in the turbines, the Mach number at the middle-span section is presented in figure 3.

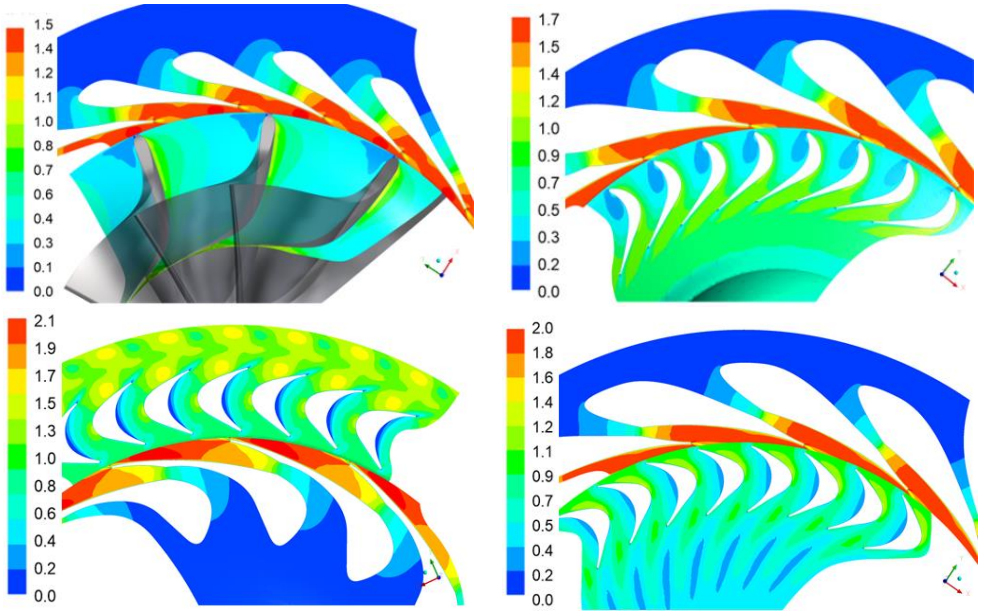

Figure 3: Mach number at 50% span

5.2 Power and efficiency under partial load

The turbine stages were analyzed under the part load operation at approximately 80%, 60% and 40% of the nominal power by means of adjustment of the turbine inlet and outlet pressure. Inlet total temperature was kept fixed as 433.15 K. The rotational speed at the part load was modified to keep u/C_0 ratio constant. The main results are summarized in table 3. A plot of the turbine power output versus the inlet total pressure is presented in figure 4. An interesting fact is that the centrifugal turbine keeps its efficiency over a wide range of the operating conditions.

Table 4 provides the details on the centrifugal turbine performance. At the design point and 80% of the rated power (2.0 MPa inlet pressure) centrifugal turbine exhibits the equal efficiency. In doing so, the nozzle velocity ratio φ remains almost the same, while the outlet velocity losses and the impeller velocity ratio are contributing to the overall loss balance so that the efficiency remains the same. Then, at 60 and 40% of the nominal power the impeller velocity ratio ψ shows a downward trend which is the main cause of the efficiency decrease. In order to give a quantitative assessment on how

φ, ψ and the outlet velocity losses affect the efficiency of the centrifugal turbine an equation $\eta_{t\text{-}s}=f(\varphi, \psi, \rho, u/C_0)$ provided for instance by Song *et al.* (2017) has to be analyzed, which is out of the scope of the current research.

Table 3: Design and part load results

Parameters			Radial inflow turbine		Centripetal turbine		Centripetal impulse turbine		Centrifugal turbine	
u/C_0			0.68		0.60		0.47		0.47	
Inlet total pressure, MPa	*Outlet static pressure, MPa*	*G, kg/s*	$\dot{W}$, *kW*	η_{t-s}	$\dot{W}$, *kW*	η_{t-s}	$\dot{W}$, *kW*	η_{t-s}	$\dot{W}$, *kW*	η_{t-s}
2.45	0.275	7.32	297.8	0.895	283.3	0.86	262.6	0.79	264.2	0.80
2.00	0.252	5.82	235.2	0.89	220.7	0.84	202.7	0.72	210.0	0.80
1.60	0.237	4.57	174.1	0.87	158.5	0.80	145.1	0.71	154.2	0.78
1.25	0.231	3.52	117.7	0.84	108.9	0.78	87.4	0.62	105.6	0.75

Table 4: Centrifugal turbine performance

Inlet total pressure, MPa	*Outlet static pressure, MPa*	H_0, *J/kg*	p_1,*MPa*	η_{t-s}	φ	c_2, *m/s*	ψ
2.45	0.275	45460	0.301	0.80	0.96	74.1	0.97
2.00	0.252	45510	0.231	0.80	0.95	68.4	0.93
1.60	0.237	43760	0.195	0.78	0.95	67.9	0.88
1.25	0.231	40060	0.173	0.75	0.95	67.7	0.80

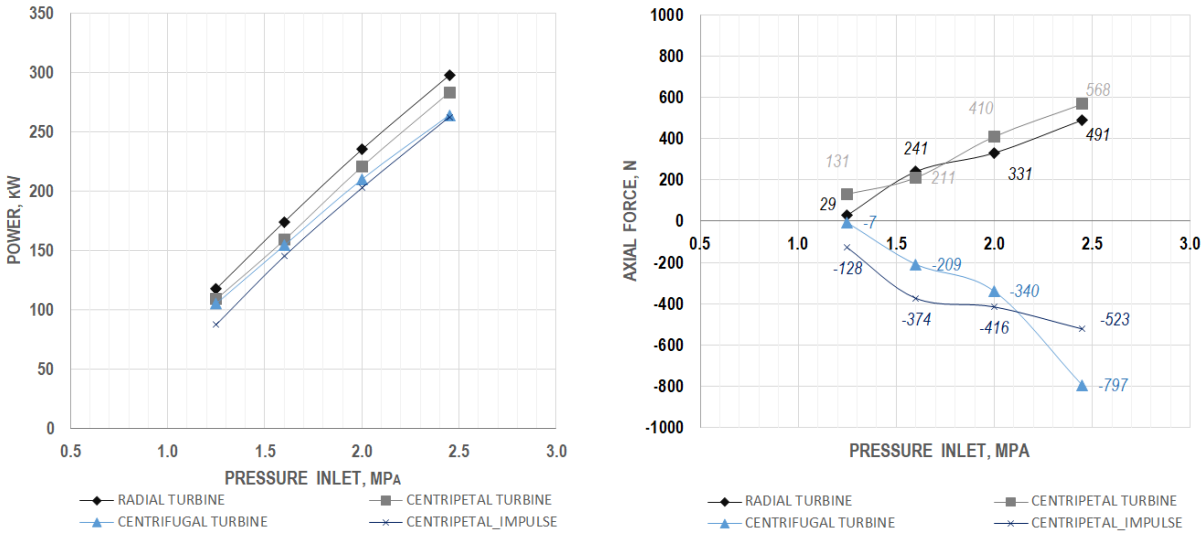

Figure 4: Left – The power output versus the total inlet pressure, Right – The axial force versus the total inlet pressure

5.3 Axial thrust

The axial force was measured on the impellers' surfaces as shown in figure 5. The magnitudes of the forces are presented in the table 5 and at the plot of the axial force versus the turbine inlet pressure. The radial inflow and centripetal turbines even despite their reaction nature demonstrate acceptable values of the thrust due to the compensation between the impeller hub and the disk back forces as seen in figure 6. An important role of the back disk labyrinth in this compensation should be outlined. Its diameters, number of fins and effective clearances have significant impact on the static pressure distribution and, hence, on the force produced. The running seal clearances may be strongly affected by the thermal deformations and the strain-stress state of the impeller. Consideration of these factors may improve the thrust prediction accuracy.

The centripetal impulse turbine with the same design of the back disk seal is producing higher thrust of 763 N and the force direction is opposite to the one of the reaction turbines. The reason is that due to the lower pressure at the impeller inlet the compensation capability of the disk's back surface is lowered. In order to fix this issue the disk back seal is modified by decreasing its inner and outer diameters by 9 mm. The number of fins and the clearance remained unchanged. In doing so, all the area between the labyrinth outer diameter and the impeller inlet diameter is kept under higher pressure which produces higher compensating force. As a result, at the full load turbine has developed 523 N of the axial thrust.

In case of the impulse centrifugal turbine its back disk surface does not provide any equilibration of the force as seen from figure 5. The unloading holes added have decreased the axial force by 30%, however, the final value was still high having reached almost 800N. All the turbines in consideration are exhibiting the thrust relief while the mass flow is decreasing.

Table 5: Produced axial force

Parameters			**Radial turbine**	**Centripetal turbine**	**Centripetal impulse turbine**	**Centrifugal turbine**
Inlet Total pressure, MPa	*Outlet Static pressure, MPa*	*G, kg/s*	*Axial force, N*			
2.45	0.275	7.32	**+491**	**+569**	**-523**	**-797**
2.00	0.252	5.82	**+331**	**+410**	**-416**	**-340**
1.60	0.237	4.57	**+271**	**+211**	**-374**	**-209**
1.25	0.231	3.52	**+29**	**+131**	**-128**	**-7**

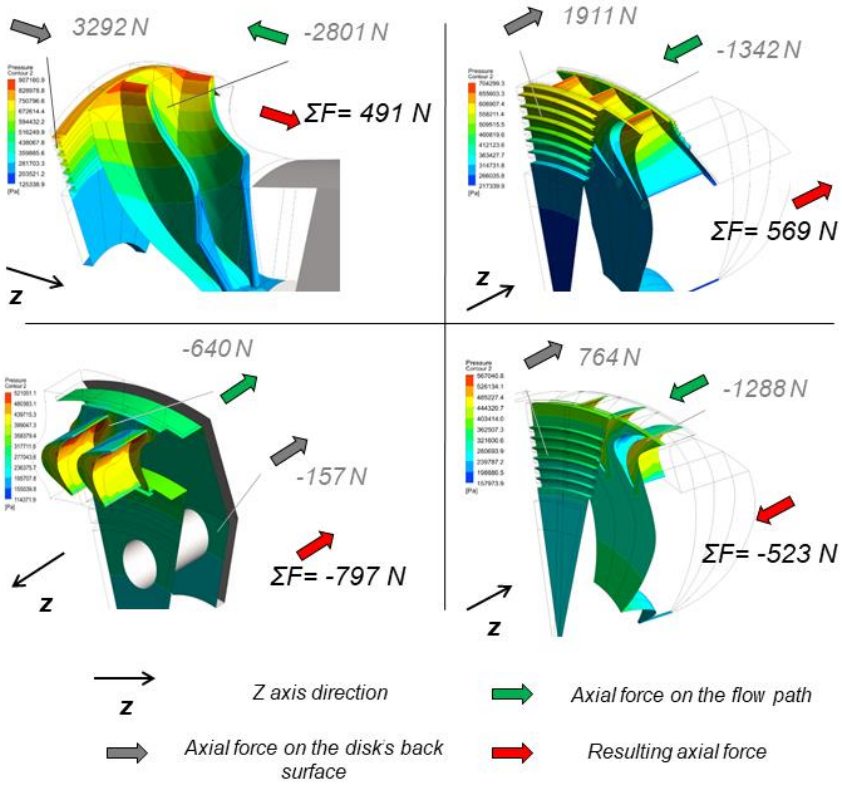

Figure 5: Static pressure distribution on the impeller surfaces

Axial force limits

Typically, in high-speed ORC turbines the radial forces do not pose challenges for the bearings due to relatively small mass of the rotor. The axil thrust instead may significantly reduce the bearing lifetime. In accordance with the experience of Zuccato Energia Srl, for the rotational speed of 25 000 rpm, commercial ball bearings with ceramic spheres may provide at least 10 000 hours of operation within the axial force of maximum 500−650 N. Therefore, commercial ceramic ball bearings available nowadays are suitable for the turbine prototypes studied in this research. Hydrodynamic or active magnetic bearings are able to withstand even higher thrusts if their usage is economically feasible.

6 CONCLUSIONS

Four radial turbines of different types were compared in terms of their efficiency and produced axial force. The turbines were designed for the similar boundary conditions in terms of the pressure, the temperature and the mass flow with using 1D meanline approach. However, the diameter and the rotational speed were selected specifically for each of them to provide the best performance taking into account different turbine reaction. The stages then were subjected to a manual 3D CFD improvement procedure to reach the design reaction and ensure the best efficiency. The performance and axial thrust were compared at full load and 80, 60 and 40 percent of the full power.

The radial inflow turbine provided the highest efficiency at the full and part load within reasonable axial forces. 1.8% of the efficiency was contributed by the exhaust diffuser. The centripetal reaction turbine was 4 to 6% less efficient in the overall considered range of the performance. The impulse turbines exhibited relatively poor efficiency, having demonstrated $\eta_{t\text{-}s}$ 11% less which corresponds to at least 30kW lower power output at the design point. At the part load operation the centrifugal impulse turbine kept its efficiency almost constant in a wide range of the operating conditions ($0.75< \eta_{t\text{-}s} <0.80$), while the centripetal impulse turbine significantly worsened its performance with the inlet pressure decrease ($0.62< \eta_{t\text{-}s} <0.79$).

The radial inflow and both centripetal stages have exhibited admissible axial forces due to their capability to balance the force by means of the disk back seal. Instead, the centrifugal impulse stage failed to provide the balancing, which resulted in higher values of the axial thrust even despite an impulse nature of this stage. It is necessary to remember that the quantitative results of CFD force assessments are to be interpreted with a reasonable safety margin.

The impulse turbines, having an advantage of the manufacturing simplicity, however, showed lower efficiency at both nominal and partial loads. In doing so, the centrifugal impulse turbine has exhibited also the highest values of the axial thrust. The radial inflow turbine remains an attractive solution due to the highest efficiency and a reasonable axial thrust at the full and part load.

NOMENCLATURE

kW	Kilowatt	
ORC	Organic Rankine Cycle	
u/C_0	stage velocity coefficient	
G	mass flow rate	kg/s
H_0	isentropic enthalpy drop	kJ/kg
l	blade height	mm
n	rotational speed	rev/min
p	pressure	Pa
T	temperature	K
$y+$	dimensionless first boundary layer element height	
$\eta_{t\text{-}s}$	total-to-static efficiency	
ρ	stage reaction	
φ	nozzle velocity ratio	
ψ	impeller velocity ratio	

Subscript

0	turbine inlet	1	nozzle outlet
2	impeller outlet	tot	total parameters

ACKNOWLEDGEMENT

The simulations have been carried out using Peter the Great Saint-Petersburg Polytechnic University Supercomputing Center. The authors appreciate technical support provided by Supercomputer center's team and by Eugeny Petukhov in particular.

Authors would like to express appreciation to Zuccato Energia Srl for the consultations on the mechanical design and part load operation aspects as well as discussion of the results.

REFERENCES

Al Jubori A., Al-Dadah R., Mahmoud S., Daabo A., 2017, Modelling and parametric analysis of small-scale axial and radial-outflow turbines for Organic Rankine Cycle applications, *Applied Energy*, vol. 190: p. 981-996.

Bülten B., Althaus W., Weidner E., Stoff H., 2015, Experimental and numerical flow investigation of a centripetal supersonic turbine for Organic Rankine Cycle applications, *Proc. of 11th Europ. Conf. on Turbomachinery Fluid dynamics & Thermodynamics ETC11*: ETC2015-088.

Kim J., Kim D., 2020, Preliminary design and off-design analysis of a radial outflow turbine for Organic Rankine Cycles, *Energies*, vol. 13, no. 8: 2118.

Klonowicz P., Surwiło J., Witanowski Ł., Suchocki T., Kozanecki Z., Lampart P., 2015, Design and numerical study of turbines operating with MDM as working fluid, *Open Engineering*, vol. 5, no. 1, https://doi.org/10.1515/eng-2015-0050

Liu Y., Huang D., 2019, Design and performance analysis of an ORC transonic centrifugal turbine, *J. Mech Sci Technol*, vol. 33: p. 1417–1430.

Mondejar M, McLinden M., Lemmon, E., 2015, Thermodynamic Properties of trans-1-chloro-3,3,3-Trifluoropropene (R1233zd(E)): Vapor Pressure, P-rho-T Data, Speed of Sound Measurements and Equation of State, *J. Chem. Eng. Data*, vol. 60: p. 2477-2489.

Moroz L., Kuo C., Guriev O., Li Y., Frolov B., 2013, Axial Turbine Flow Path Design for an Organic Rankine Cycle Using R-245fa, *Proc. of the ASME Turbo Expo 2013: Turbine Technical Conference and Exposition*, vol. 5A: V05AT23A004, https://doi.org/10.1115/GT2013-94078

Sebelev A., Scharf R., Zabelin N., Smirnov M., 2015, Design and numerical analysis of processes in siloxane vapor driven turbine, *of the 3rd Int. Seminar on ORC Power Systems*: Paper ID44.

Sebelev A., Smirnov M.,. Kuklina N., Lapshin K., Laskin A., 2019, Comparison of the cubic equations of state and different transport properties models for orc turbines modeling, *Proc. of 13th Europ. Conf. on Turbomach. Fluid dynamics & Thermodynamics ETC13*: ETC2019-141.

Song Y., Sun X., Huang D., 2017, Preliminary design and performance analysis of a centrifugal turbine for Organic Rankine Cycle (ORC) applications, *Energy*, vol. 140, no. 1: p. 1239-1251.

Tiainen J., Jaatinen-Värri A., Grönman A., Sallinen P., Honkatukia J., Hartikainen T., 2021, Validation of the Axial Thrust Estimation Method for Radial Turbomachines, *Int. J of Rotating Machinery*, vol. 2021: 6669193.

Weiß A., Hauer J., Popp T., Preißinger M., 2017, Experimental investigation of a supersonic micro turbine running with hexamethyldisiloxan, *AIP Conference Proceedings*, 1889, 020050.

Weiß A., Popp T., Müller J., Hauer J., Brüggemann D., Preißinger M., 2018, Experimental characterization and comparison of an axial and a cantilever micro-turbine for small-scale Organic Rankine Cycle, *Applied Thermal Engineering*, vol. 140: p. 235-244.